Nanoparticle deposition in hydrogenated amorphous silicon films during rf plasma deposition

D. M. Tanenbaum,[a] A. L. Laracuente, and Alan Gallagher[b]
JILA, National Institute of Standards and Technology and University of Colorado, Boulder, Colorado 80309-0440

(Received 13 October 1995; accepted for publication 22 January 1996)

Particles of 2–14 nm diameter, representing 10^{-4}–10^{-3} of the film volume, are observed by scanning tunneling microscopy (STM) in thin films of hydrogenated amorphous silicon (*a*-Si:H) grown by rf-plasma-enhanced deposition using optimized conditions. The particles are produced in the discharge and incorporated in the film during growth, in contradiction to expected particle trapping by discharge sheath fields. The interfaces between the nanoparticles and the homogeneous film can produce low-density regions that form electronic defects in *a*-Si:H films. © *1996 American Institute of Physics.* [S0003-6951(96)04812-4]

Particle formation in rf plasmas used for chemical vapor deposition and dry-etching processing can degrade or destroy wafers or thin film devices if the particles reach the substrate. Consequently, there have been extensive studies on the formation and behavior of particles in plasmas, particularly those containing silicon or silane.[1–7] The basic picture that has emerged is that negative ions of silicon-containing molecules are formed by electron attachment, and they grow by reactions with silicon-containing radicals and cations. Because electron velocities are much greater than cation velocities, the growing particle becomes negatively charged until a surface potential of several volts yields a balance between the average particle charging rate by electrons and cations. The net current from the bulk plasma to the discharge electrodes must also be zero on average, and the plasma thereby becomes positively biased by a ''plasma potential'' of approximately the peak rf voltage. This voltage appears across the ''sheaths''—the dark regions adjacent to the electrodes—and at the discharge edges. The negatively charged particles are thereby trapped in the bulk plasma by electrostatic forces, and they cannot reach the electrodes while the discharge is operating. Once they grow to $\sim\mu$m size, particles can escape the downstream end of a parallel plate discharge, where viscous drag forces ($\propto d^{\,2}$, where d is the particle diameter) overcome electrostatic forces ($\propto d$). This absence of particle deposition *during* film growth implies that bulk film properties do not result from particle incorporation. We demonstrate here that this picture is incorrect; small particles do reach the substrate during the discharge. These nanoparticles are too small to create short circuits between layers, but probably have significant effects on film properties, creating defects and voids along their interfaces with the surrounding film.

Thin films of *a*-Si:H have a wide range of practical applications, such as photovoltaic modules, thin-film transistors in flat-panel displays, and 3-color detectors in imaging systems. Although *a*-Si:H films can be grown under a wide variety of conditions, the best, or ''device quality,'' photovoltaic films are typically grown in low-power, parallel-plate rf discharges in silane or silane diluted with hydrogen. The present discharge chamber and conditions closely mimic those required for optimum film growth.

Electron microscopy studies with a few nm resolution find that ''device quality'' material is homogeneous.[8–10] Consistent with this, *in situ* ellipsometry suggests that initial nucleation is dependent upon the substrate, but is followed by homogeneous film growth beneath a thin, H-rich surface layer.[11] However, on a $\leqslant$1 nm scale, voids or low density regions are observed in *a*-Si:H by small-angle x-ray scattering (SAXS),[12] and pockets of clustered H atoms are observed in NMR measurements.[13] These regions are suspected to play a role in carrier recombination and may also be connected with certain types of Si-H bonds that have been suggested as causing the light-induced defects in *a*-Si:H photovoltaic cells.[14] These metastable defects show annealing behavior similar to that for hydrogen migration and have also been correlated with both SAXS and infrared absorption measurements of Si–H bonds.[15] The causes of these inhomogeneous regions have been unknown; here we find that continuous, small-particle deposition could be responsible.

Plasma particulate studies have so far detected particles suspended in the plasma or collected on surfaces downstream or after the plasma is extinguished, by using light-scattering or Langmuir probe measurements of plasma particles,[6] or SEM or TEM measurements of collected particles.[2] Such measurements do not ascertain if particles reach the surface during film growth. Here we measure the film surface with an STM and conclude from the statistics and shapes of detected particles that they are deposited during film growth.

Details of our experimental apparatus have been described in previous publications.[16] An ultrahigh-vacuum (UHV) analysis chamber is directly connected to a small film-deposition chamber, where the substrate is centered in the grounded electrode of an rf, parallel plate discharge between 5 cm square electrodes spaced by 1.9 cm. The temperature of the entire chamber is $\sim$250 °C during all film depositions, the silane pressure is $\sim$72 Pa, the film deposition rate is 0.1–0.2 nm/s, and $\sim$5% of the silane is depleted by the discharge.

[a]Present address: School of Applied and Engineering Physics, Cornell University, Ithaca, NY 14853.
[b]Member, Quantum Physics Division, National Institute of Standards and Technology. Electronic mail: alang@jila.colorado.edu

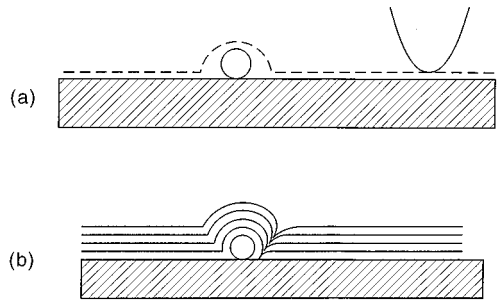

FIG. 1. (a) An example of a constant-gap STM scan of the tunneling probe and a spherical particle. (b) Film surface shape as successive film layers conformally deposit (left side of particle). On the right side of the particle an extended void due to partial shadowing is indicated.

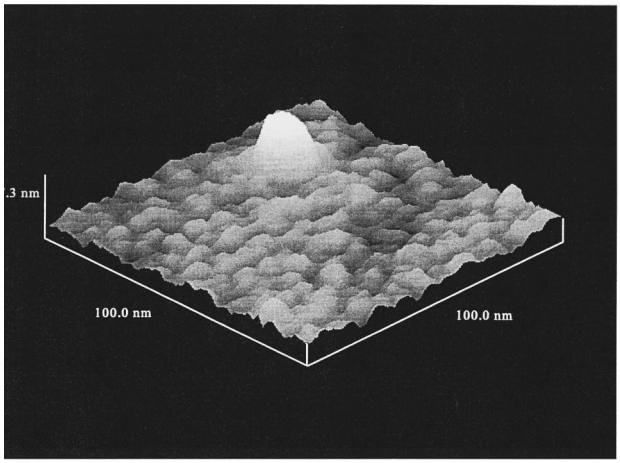

FIG. 2. STM image of a nanoparticle on a 4.2-nm-thick *a*-Si:H film.

STM probes, made from etched W or PtIr wire, were heated in vacuum prior to tunneling on *c*-Si surfaces, where sharp Si nanocolumns are constructed on the substrate and probe tip[17] to achieve high-resolution tunneling of high-angle surface features. The nanocolumn used here had <2 nm tip radius of curvature and 45–70° taper over the final 5 nm. A spherical particle on a flat film surface will appear as a smoothly rising bump in an STM image, as shown in Fig. 1. Note that the measured width is broadened by twice the tunneling gap plus the width of the probe tip, whereas the height of the feature remains an accurate measure of the diameter of a spherical particle. As also shown in Fig. 1, film deposition over a particle preserves height and expands feature width.

The substrates were Si(100) wafers that were heated in UHV to $\sim$1050 °C to remove oxide and contaminants, resulting in a 2×1 dimer reconstruction and a typical rms roughness, σ, of 0.05 nm. Each substrate was examined by STM prior to film growth to verify flatness, then transferred in vacuum to the deposition chamber, coated with *a*-Si:H film, and returned in vacuum for STM analysis. Tunneling currents on *a*-Si:H were 20–60 pA with a negative 3–6 V sample bias, as is required by the very low conductivity of intrinsic to *a*-Si:H. A measured exponential decay in the tunneling current with increasing probe-sample separation confirms we are tunneling above the films.

The films used in this study are $\leqslant$50 nm thick and have homogeneous distributions of hills and valleys over the majority of the film surface,[18] with $\sigma = 0.3$–0.5 nm for the film thicknesses reported here. The reported nanoparticles are distinguished from this background roughness by their heights, which exceed 10σ. Figure 2 shows an image of a nanoparticle on a 4.2 nm thick *a*-Si:H film. This requirement of clear contrast with the background film roughness sets a lower limit of $\sim$2 nm on the reported particle sizes.

We report here on a total of $\sim$30 particles observed on the surfaces of six films, of 1–50 nm thickness. Typically $\sim$20 randomly selected areas of 100 nm$\times$100 nm were scanned on each surface. The nanoparticles appear circular, so we describe them by their height and FWHM width in the STM images. Figure 3 shows the distribution of particle heights, the surface number density of particles, and the average feature width/height as a function of film thickness. The trend toward lower width//height for thicker films is consistent with burial of these nanoparticles beneath subsequently deposited *a*-Si:H film, as shown in Fig. 1(b). (Either the resulting conformal film coverage or extended void growth shown there may occur, depending on the extent of radical surface diffusion before incorporation,[8,19] but this is not discerned in the STM image.) A range of width/height values was observed for each film; these were consistent with spherical particles distributed throughout the film, convolved with our probe resolution.

It is possible that particulates from the chamber surfaces could deposit on the samples during sample transfer into the STM, or discharge particulates may deposit on the substrate after discharge termination. The following observations show that these are not the source of the detected particulates: (1) Such particulates will not be well adhered to the film surface, and the STM probe would be unlikely to scan smoothly and repeatedly over them, as occurred in all images. (2) A much larger range of particle size exists in the discharge, particularly larger particles. (3) The recorded bumps are round, but particularly with increasing film thickness their aspect ratios are lower than that expected for spherical particles scanned by our STM probe, whose resolution is known from STM measurement of a Si nanocolumn. This is consistent with the width broadening by film growth over a spherical particle, as shown in Fig. 1(b). (4) The observed increase in particle density with increasing film thickness (Fig. 3) is only con-

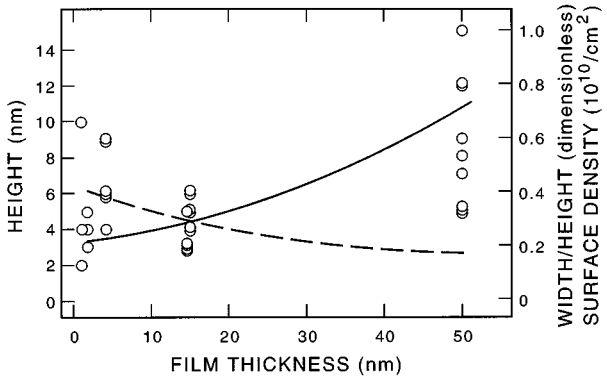

FIG. 3. Measured particle heights (open circles), average particle surface density (solid line), and average height/width ratios (dashed line). The indicated surface density of the 50 nm film is 1.4$\times$ the measured density, to correct for 2–3 nm particles missed on this rougher surface.

sistent with a steady deposition of particulates. (5) For each of two 15-nm-thick films, one grown in two successive discharges and the other in six consecutive discharges, five nanoparticles were observed in the same total area. Similarly, the thickest (50 nm) film was grown with a single discharge termination, yet it had the highest number density of nanoparticles.

A second possible source of the observed bumps might be initial growth islands, arising before the substrate surface is covered by *a*-Si:H. Several types of evidence rule this out. (1) The observed bumps fill a very small fraction of the surface area, and they are surrounded by much smoother film, which is inconsistent with film growth from initial islands. (2) The homogeneous roughness seen on the thinnest (1 nm) films demonstrates that the entire surface is fully covered with *a*-Si:H by this thickness, yet we see increasing bump density with additional deposition. (3) The observed range of feature width/height values is consistent with spherical particles covered by varying portions of the *a*-Si:H film, not initial islands covered by the remaining film. (4) We observed similar size particles in thin *a*-Si:H films grown on vacuum-cleaved GaAs, although we did not collect statistics on these.

Our data suggest the total volume fraction of nanoparticles in the *a*-Si:H film is between 10^{-3} and 10^{-4}. (If voids propagate from these particles, as indicated in Fig. 1(b), these could affect a larger film volume.) It is possible that this fraction is highly dependent on details of our deposition chamber; measurements of particles in plasmas have shown that they are extremely sensitive to specific geometric, electrical, and gas-flow features of the reactor. One very significant factor is that many *a*-Si:H deposition systems directly heat only the substrate electrode, and this provides a thermophoresis force driving particles away from the substrate. In our system, the heating is more uniform, resulting in a decrease in thermophoresis forces.

It is interesting to speculate why these particles are reaching the substrate during the discharge, in spite of the average negative charge (N) of about 5–40 electrons predicted for 2–15 nm particles.[7] A particle must be neutral or positively charged to pass through the discharge sheath, and random charge fluctuations of $\sim N^{1/2}$ are grossly insufficient for this. However, particles collect close to the plasma-sheath boundary because of ion-drag forces, and if they achieve sufficient density in this region the local electron density becomes severely reduced, leading to a reduction in N and a significant fraction of temporarily neutral particles. Some of these will diffuse into the sheath, but diffusive drift is so slow that almost all will attach a sheath electron and be returned to the plasma-sheath boundary region. But occasionally a sheath cation will attach before an electron, and this positively charged particle will drift so quickly to the substrate, in the strong sheath field, that it is unlikely to encounter an electron. We estimate that this could produce a particle flux comparable to that observed here.

Recently, Wanka *et al.*[20] have used atomic force microscopy and Kazuyiki *et al.*[21] have used STM to examine thin *a*-Si:H films grown from silane discharges. They observed similar bumps on their early growth surfaces but interpreted them as initial island growth. As shown above, this is not the case here, and it probably is not the case in their films either. Schmidt *et al.* have shown that particle buildup in the plasma affects *a*-Si:H film ellipsometry signals.[22] Here we have shown that this is probably due to actual particle incorporation into the films, as opposed to a changed mixture of depositing molecules. These particles are incorporated into the *a*-Si:H film for discharge conditions that yield optimal properties, and yet they must be limiting the homogeneity and electronic properties. Thus, significant improvement in *a*-Si:H electronic properties may still be possible.

This work was supported by the National Renewable Energy Laboratory, under contract DAD-4-14084-01.

[1] The April 1994 issue of Plasma Science is a special issue on charged dust in plasmas.
[2] L. Boufendi, A. Plain, J. P. Blondeau, A. Bouchoule, C. Laure, and M. Toogood, Appl. Phys. Lett. **60**, 169 (1992).
[3] A. Garscadden, Pure & Appl. Chem. **66**, 1319 (1994).
[4] A. A. Howling, L. Sansonnens, J. L. Dorier, and C. Hollenstein, J. Appl. Phys. **75**, 1340 (1994).
[5] J. Perrin, P. Molinês-Mata, and P. Belenguer, J. Phys. D **27**, 2499 (1994).
[6] Y. Watanabe and M. Shiratani, Jpn. J. Appl. Phys. **32**, 3074 (1993).
[7] J. E. Daugherty, R. K. Porteous, M. D. Kilgore, and D. B. Graves, J. Appl. Phys. **72**, 3934 (1992).
[8] C.-C. Tsai, J. C. Knights, G. Chang, and B. Wacker, J. Appl. Phys. **59**, 2998 (1986).
[9] J. C. Knights and R. A. Lujan, Appl. Phys. Lett. **35**, 244 (1979).
[10] J. C. Knights, Mater. Res. Soc. Symp. Proc. **38**, 371 (1985).
[11] Y. M. Li, I. An, H. V. Nguyen, C. R. Wronski, and R. W. Collins, Phys. Rev. Lett. **69**, 2814 (1992).
[12] J. Shinar, H. Jia, R. Shinar, Y. Chen, and D. L. Williamson, Phys. Rev. B **50**, 7358 (1994).
[13] J. Baum, K. K. Gleason, A. Pines, A. N. Garroway, and J. A. Reimer, Phys. Rev. Lett. **56**, 1377 (1986).
[14] M. Stutzmann, W. B. Jackson, and C. C. Tsai, Phys. Rev. B **32**, 23 (1985).
[15] S. Guha, J. Yang, S. Jones, Y. Chen, and D. Williamson, Appl. Phys. Lett. **61**, 1444 (1992).
[16] G. C. Stutzin, R. M. Ostrom, A. Gallagher, and D. M. Tanenbaum, J. Appl. Phys. **74**, 91 (1993).
[17] R. M. Ostrom, D. M. Tanenbaum, and A. Gallagher, Appl. Phys. Lett. **61**, 925 (1992).
[18] D. M. Tanenbaum, A. Laracuente, and A. C. Gallagher (unpublished).
[19] J. R. Abelson, Appl. Phys. A **56**, 493 (1993).
[20] H. N. Wanka, A. Hierzenberger, and M. B. Schubert (unpublished).
[21] I. Kazuyiki, K. Tanaka, S. Yamasaki, K. Mii, and A. Matsuda, Appl. Phys. Lett. **65**, 1760 (1994).
[22] U. I. Schmidt, B. Schroder, and H. Oechsher, J. Cryst. Growth **164-166**, 127 (1993).